K-edge x-ray dichroism investigation of $Fe_{1-x}Co_xSi$: experimental evidence for spin polarization crossover

G. R. Hearne[1 *] , G. Diguet[1 ¥] , F. Baudelet[2], J-P Itié[2] and N. Manyala[3]

[1]Department of Physics, University of Johannesburg, P.O. Box 524, Auckland Park, 2006, Johannesburg, South Africa

[2]Synchrotron SOLEIL, L'Orme des Merisiers, Saint-Aubin, BP 48, 91192 Gif-sur-Yvette Cedex, France

[3]Department of Physics and Institute of Applied Materials , University of Pretoria , Private Bag X20, Hatfield , 0028, Pretoria, South Africa

[*] Corresponding author : grhearne@uj.ac.za

[¥] Current address : Institut Néel, CNRS and Université Joseph Fourier, 5 rue des Martyrs BP166 , 38042 Grenoble Cedex 9, France

Abstract : Both Fe and Co *K*-edge x-ray magnetic circular dichroism (XMCD) have been employed as element-specific probes of the magnetic moments in the composition series of the disordered ferromagnet $Fe_{1-x}Co_xSi$ (for x = 0.2, 0.3, 0.4, 0.5). A definitive single peaked XMCD profile occurs for all compositions at both Fe and Co *K*-edges. The Fe 4*p* orbital moment, deduced from the integral of the XMCD signal, has a steep dependence on x at low doping levels and evolves to a different (weaker) dependence at $x \geq 0.3$, similar to the behavior of the magnetization in the Co composition range studied here. It is systematically higher, by at least a factor of two, than the corresponding Co orbital moment for most of the composition series. Fine structure beyond the *K*-edge absorption (limited range EXAFS) suggests that the local order (atomic environment) is very similar across the series, from the perspective of both the Fe and Co absorbing atom. The variation in the XMCD integral across the Co composition range has two regimes, that which occurs below x=0.3 and then evolves to different behavior at higher doping levels. This is more conspicuously present in the Fe contribution. This is rationalized as the evolution from a half-metallic ferromagnet at low Co doping to that of a strong ferromagnet at $x > 0.3$ and as such, *spin polarization crossover occurs*. The Fermi level is tuned from the majority spin band for $x < 0.3$ where a strongly polarized majority spin electron gas prevails, to a regime where minority spin carriers dominate at higher doping. The evolution of the Fe-derived spin polarized (*3d*) bands, indirectly probed here via the *4p* states, is the primary determinant of the doping dependence of the magnetism in this alloy series.

Keywords : half-metallic magnet ; FeSi-Co ; K-edge XMCD ; strong ferromagnet ; spin polarization ;

PACS number(s): 72.25.Ba , 75.25.-j, 75.50.Bb

1. Introduction

End-member monosilicides FeSi and CoSi are not magnetic. They have the cubic B20 structure (NaCl (B1) structure derivative) in which the transition-metal has seven neighboring silicons [1]. Chemical substitutions may occur across the entire series without changing the cubic B20 crystal structure or nucleating secondary phases [2]. Moreover, the doped $Fe_{1-x}Co_xSi$ alloys in a wide concentration range $0.05 \leq x \leq 0.8$, become disordered metallic helical magnets with a long helix period [2-5], which unravels from a conical to ferromagnetic state in low applied fields of less than 0.2 T [4, 6].

Negative magnetoresistance behavior confined to a narrow region of the spin-ordering temperature T_C is anticipated in such an itinerant magnetic system. This is exemplified by the case of MnSi, wherein the application of an external field is supposed reduce the spin disorder and associated scattering from these fluctuations in the vicinity of T_C [7]. However these Co doped magnetic alloys show unusual positive magnetoresistance, over a wide temperature range encompassing T_C. This is attributed to quantum interference effects as a result of the disorder [7], although this is still a matter of controversy [4]. Furthermore there is intense interest in this alloy series because of the possibility of forming a silicon-based magnetic semiconductor for spintronics applications [8-10].

The intriguing end-member semiconductor FeSi has been investigated for decades because of the unusual temperature dependent magnetic susceptibility, attributable to strong electron correlation effects [11]. Upon Co doping the small gapped (Δ~50 meV) FeSi becomes metallic and magnetic. T_C increases monotonically in $Fe_{1-x}Co_xSi$ up to a doping level x=0.4 which has the highest value T_C ~53 K and then decreases at higher doping levels $x > 0.4$ [4, 7]. The origin of the magnetism as invoked by the Co-doping is still an outstanding question.

To tackle this we probe the magnetic moment speciation on both Fe and Co sites as a function of Co composition for x= 0.2, 0.3, 0.4 and 0.5 in the $Fe_{1-x}Co_xSi$ composition series. We are aware of only limited previous work in this area involving ^{57}Fe Mössbauer spectroscopy and ^{59}Co NMR studies which indicates that both a Fe and Co moment is existent. The Co moment decreases as a function of increasing Co composition (for x=0.2 to x=0.6), whereas the Fe moment peaks at x=0.4 [12].

We use an alternative atomic probe of the moment speciation in this interesting alloy series, viz, x-ray magnetic circular dichroism (XMCD) at both the Fe and Co *K*-edges. This

renders it an *element-specific probe* with a higher *bulk sensitivity* of magnetic-electronic properties than *L*-edge dichroic measurements In so doing an indication of the spin and primarily orbital moment contribution or variation in the alloy series is obtained. In addition this provides the first experimental probe of the electronic band structure near the Fermi level (E_F) over a wide composition range [13]. The compositions , x = 0.2, 0.3, 0.4 and 0.5, were selected to cover a comparatively wide range of doping. This was intended to include the regime where there is a near linear dependence of T_C and saturation magnetization on Co concentration at $x \leq 0.3$, as well as higher doping levels where there is a drastic change to the composition dependences of these quantities. This encompasses a Co doping level where T_C and saturation magnetization reach their maximum values (viz, x = 0.4) [4, 7]. The outcomes could plausibly serve as useful input to *ab initio* calculations of the electronic band structure as well as to rationalize the appreciable change in the composition dependence of the magnetic behavior that occurs in the vicinity of x = 0.3.

The *K*-edge absorption signal arises from electric dipole transitions from the 1*s* core level to the unoccupied 4*p* conduction band levels of the absorbing atom [14]. These 4*p* orbitals are hybridized with the 3*d* orbitals of both the absorbing atom and those from the surrounding local atomic environment. A significant contribution to the *K*-edge dichroism is from the polarization dependent transition intensities of the excited photoelectron to spin-orbit perturbed *p*- and *d*- states of the hybridized *3d-4p* conduction band [15, 16]. The integral of the XMCD signal is proportional to the expectation value of the 4*p* *orbital angular momentum*,$\langle L_Z \rangle_P$ [16-18] . This stems from the imbalance of L_Z quantum numbers $+m_l$ and $-m_l$ in the density of empty *3d*-4*p* states near E_F.[14] Such an imbalance results in the orbital moment contribution M_L to the total atomic moment :

$$M_L = \mu_B \sum_{m_l} (N_h^{+m_l} - N_h^{-m_l}) , \qquad (1)$$

where N_h is the number of holes in the (4*p*) conduction band with orbital quantum numbers $\pm m_l$.

At low Co concentrations up to x~0.25, the saturation magnetization in $Fe_{1-x}Co_xSi$ is found to rise almost linearly with Co doping, which also adds one additional electron per substituted Fe atom [7]. This behavior and the experimentally observed fast saturation of the magnetization versus external magnetic field have been explained by invoking half-metallic ferromagnetism in the composition range $0.08 \leq x \leq 0.25$ [4, 6] , consistent with electronic structure calculations [19]. This is a case where electrons in the partially filled majority spin

band are responsible for conduction whereas the minority spin band has been shifted (e.g., as a result of the exchange splitting) such that E_F resides within the gap of only the minority spin channel. The result is a nearly fully majority-spin polarized electron gas. That half metallic behavior occurs at all in such disordered alloys is considered intriguing because disorder is normally expected to smear out and destroy such electronic behavior [20].

We seek to consider what is the electronic situation prevailing at higher Co doping levels, $x \geq 0.3$, where T_C reaches a maximum. The nature of the spin polarized bands have not been subject to experimental probes in this respect and magnetic properties from band structure calculations may not be reconciled with the experimental data [19, 21]. The XMCD investigation presented here is an attempt to address this.

2. Experimental details

XMCD experiments at the *K*-edge have been performed at the ODE beamline of Synchrotron SOLEIL [22, 23]. An external field of 1.3 T has been applied along the beam direction to impose a magnetization direction (i.e., orientations of electron spin of majority/minority spin bands in the ferromagnet). The magnetic field is switched parallel and anti-parallel to the beam direction to attain the equivalent of incident x-ray photon helicities parallel and anti-parallel to the magnetization direction [24, 25]. The ODE beamline permits extremely high stability dispersive x-ray absorption spectroscopy (XAS) studies. This is an imperative for obtaining reliable *K*-edge XMCD signals, known to be small ($< 10^{-3}$) in transition metals. These are anticipated to be even weaker in the $Fe_{1-x}Co_xSi$ series where the magnetic moment is less than 0.2 μ_B per f.u. [4].

Samples are from the same batch used by Manyala et. al. [7] or have been synthesized in a similar way by arc-melting 4N pure starting materials with the prescribed ratio, followed by annealing procedures. X-ray diffraction and ^{57}Fe Mössbauer spectroscopy at ambient conditions confirmed the single-phase nature of the samples. The determination of the nominal Co concentrations was obtained from the linear dependence of lattice parameter on Co composition (Vegard's law) and in selected cases confirmed by x-ray microanalysis [2, 7].

Magnetic characterization of the alloys was performed in a SQUID magnetometer (Quantum Design : MPMS). Saturation magnetization M_0 values are taken from the high field value at ~ 4 T in the M - B curves. After zero-field cooling of the sample T_C was

obtained from the warming curves as the onset of the precipitous change in magnetization to paramagnetic behavior, similar to ref. [4].

Fine-grained powdered samples have been compacted between diamond anvils in a pressure cell cavity to ensure uniform disks of ~12 μm thickness in the ϕ~150 μm diameter cavity. The beam spot at the sample was 28 x 42 μm (FWHM). Measurements in the spin-ordered state have been taken at 4 K ($T << T_C$) in a customized cryostat. There were selected measurements at $T > T_C$, to verify collapse of the XMCD signal. Data acquisition time for the XMCD spectrum was typically 12 - 18 hours for each composition. A series of Fe *K*-edge spectra were taken followed by corresponding Co *K*-edge measurements.

3. Results

Figure 1 shows the magnetic characterizations in the series of alloys we have investigated. This has been compared with the previous experimental data of Onose et. al. [4] and Manyala et. al. [9]. The x=0.4 Co doped sample has the maximum M_0 and T_C. Our T_C curve follows quite closely that of Onose et. al. [4], whereas M_0 does show some differences at x=0.5 compared to literature values. Nevertheless our composition series has the correct trend, with the maximum M_0 being attained at x=0.4 after which there is a decreasing trend at higher compositions. Part of the reason for the difference compared to the previous literature may be varying levels of Fe/Co homogeneity from different sample preparation procedures [2, 4, 9].

Figure 2(a) shows the XMCD signal at the Fe *K*-edge. Note that the signals are weak in these small moment systems, at the level of 10^{-4} or less, but nevertheless discerned reliably. Further note that this signal is single-peaked (unipolar) in the vicinity of the *K*-edge (7112 eV), for all compositions. The XMCD profile is unlike that of ferromagnetic Fe metal, which has a positive and negative going segment at the *K*-edge [25, 26]. Instead, the Fe XMCD signal for the $Fe_{1-x}Co_xSi$ series is similar to that of Co or Ni metal ferromagnets, notably a single peak profile. This is considered in somewhat more detail in the discussion section.

Figure 2(b) also shows the XMCD signal for the Co absorbing atom across the composition series. It is more challenging to obtain a good signal-to-noise ratio in these cases. The pertinent Co signal at energies greater that ~7600 eV is in a regime where there is comparatively strong absorption of the incident x-rays (i.e., beyond the Fe *K*-edge at 7112

eV) by the Fe constituents in the sample. There are unambiguous single peaked Co XMCD signals for the composition series, similar to the case of the Fe XMCD. The x=0.2 sample signal is the most unreliable because of both the low Co content and high attenuation by the abundant Fe concentration (i.e., 80% Fe) in this alloy. The single peaked nature of the XMCD suggests that features in the Co electronic density of states near E_F are similar to the Fe component.

The XMCD signal, obtained from the difference of spin polarized absorption spectra μ^+ and μ^- [24], has been integrated and normalized to the integral of the unpolarized absorption $\mu_0 = (\mu^+ + \mu^-)/2$:

$$A_{XMCD} = \int_{K-edge} (\mu^+ - \mu^-)dE \Big/ \int_{K-edge} (\mu_0)dE \quad . \qquad (2)$$

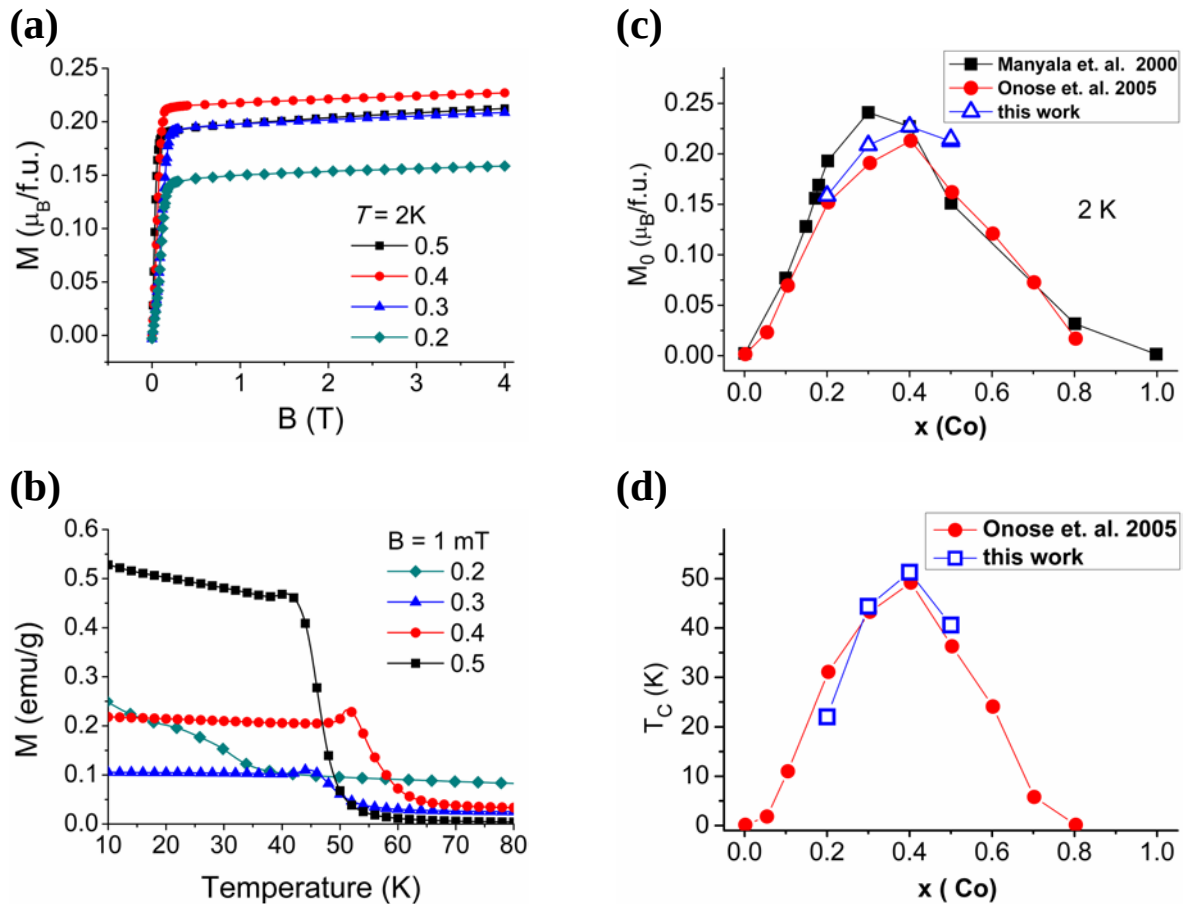

Figure 1 (colour online) : (a) Magnetization M versus applied field B and (b) M versus T for different Co concentrations x = 0.2, 0.3, 0.4 and 0.5 in the alloy series $Fe_{1-x}Co_xSi$. Symbols show (c) saturation magnetization M_0 and (d) spin-ordering temperature T_C measured for the alloys of this work, compared with the previous studies of refs [4, 7] .

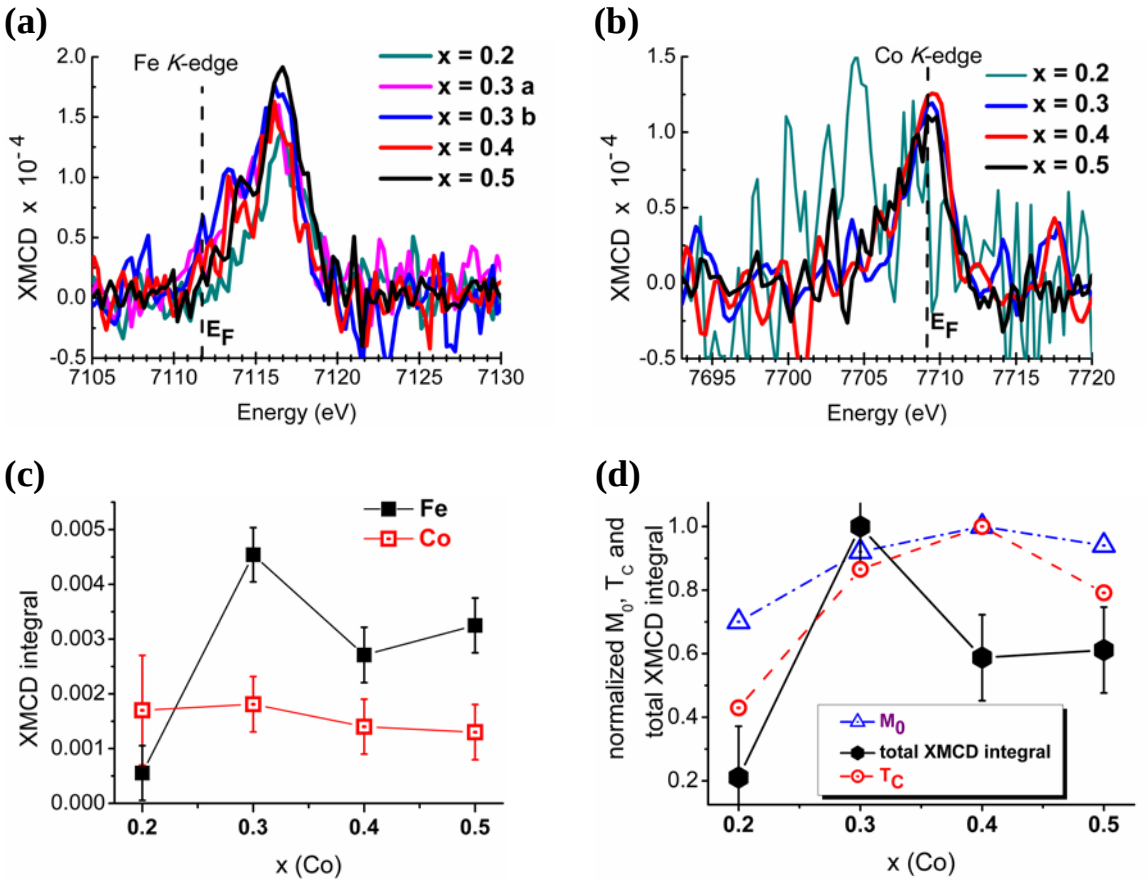

Figure 2 (colour online) : (a) and (b) panels show XMCD signal at the Fe and the Co *K*-edges, respectively, for the various compositions. Note that the XMCD signal in this small moment series is at the level of 10^{-4} . (c) Symbols show values of the integrated XMCD signals of (a) and (b), proportional to the expectation value of the 4*p* orbital angular momentum $\langle L_Z \rangle_P$ These have been normalized to the unpolarized absorption edge profile to obtain data independent of sample thickness [24]. (d) Saturation magnetization M_0, T_C and composition weighted total XMCD integral normalized to maximum values, serving to emphasize the different composition dependence regimes and locations of maxima. Solid or dashed lines are to guide the eye in (c) and (d).

Figure 2(c) shows the integral of the XMCD signal for the various Co concentrations, including error estimates [27]. It may be noted that the Fe-originated integral has a steep dependence on *x* at low doping levels and evolves to a different (weaker) dependence at $x \geq 0.3$. It is systematically higher than the corresponding Co signal for most of the composition series, by at least a factor of two. As this integral is proportional to the 4*p* orbital moment [16-18], see equation (1), it indicates that there is definitely an unquenched orbital contribution on both transition-metal components of the alloy. The dominant contribution arises from the Fe component in the alloy for most of the series of Co doping studied here.

Next nearest neighbors to the absorbing atom in the B20 structure of these disordered alloys are both Fe and Co species [1]. Information on the local atomic environment is obtained from the corresponding fine structure features in the energy range beyond the *K*-edge (limited range EXAFS) of the spectra. Figure 3 depicts that these are very similar for each composition, especially at the Fe *K*-edge. This suggests that the local crystal chemical environment around each Fe and Co atom does not vary appreciably for different compositions up to x=0.5. However, the experimental set-up for XMCD is optimized for reliable data collection only in the regime very near the absorption edge. X-ray absorption data taken to well beyond the *K*-edge would be required for a reliable EXAFS analysis, to check this supposition.

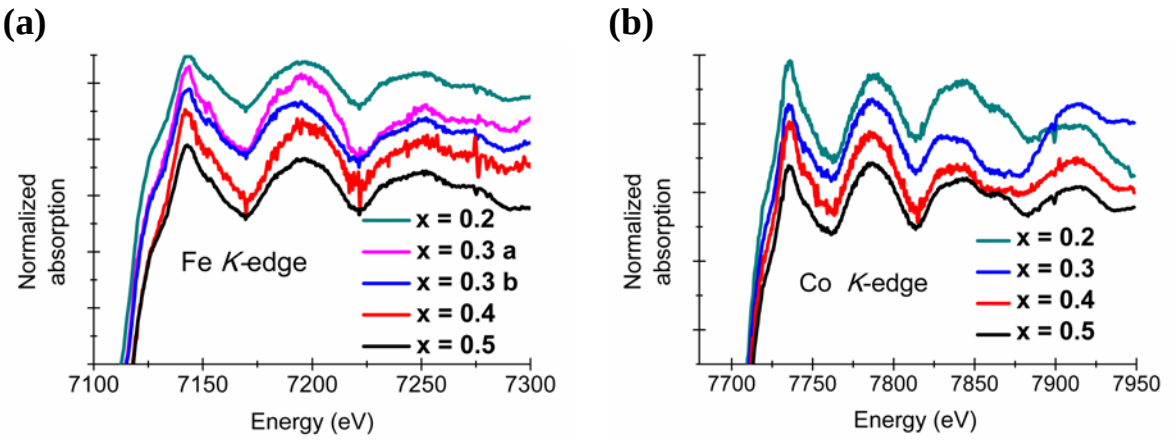

Figure 3 (colour online) : (a) and (b) panels showing limited range EXAFS at the Fe and Co *K*-edges, respectively. Spectra have been offset from each other for clarity. Some distortions of the signal are apparent in the Co spectra. These likely stem from artifacts introduced by the experimental setup optimized for near edge (XANES and XMCD) measurements.

It appears from figure 2(c) that x=0.3 marks a transition region, where the composition dependence of the orbital moment contribution changes appreciably across the series (especially for the Fe species). There appears to be a weak maximum at x=0.3, to within the error estimates obtained using the procedure mentioned in ref. [27]. Even if these error bars have been underestimated, from a consideration of statistical scatter and signal-to-noise ratio of the XMCD signals in figure 2(a), x=0.3 still represents a doping level where there is a transition to a new dependence on increasing Co composition. This should be compared with the trend of M_0 and T_C in figure 1 which for our sample exhibits a broad maximum at x=0.4 in this composition range. These quantities also exhibit a change in their composition

dependence when x is in the range 0.3 - 0.4 . Figure 2(d) shows plots of the Fe-Co composition weighted total XMCD integral, M_0 and T_C , normalized to the maximum values. It should be noted that the XMCD integral is proportional to the total 4*p* orbital moment $\langle L_Z \rangle$ only. Whereas the atomic moment contribution in M_0 and T_C involves the total atomic angular momentum J , i.e., contributions from both the orbital $\langle L_Z \rangle$ and atomic spin $\langle S_Z \rangle$ moments. Figure 2(d) is then suggestive that the composition dependence of the orbital and spin contributions are different for Co concentrations probed here.

4. Discussion

We attempt to account for the XMCD behavior depicted in figure 2, notably (i) that the XMCD profile is unipolar across the entire composition series and (ii) that there appears to be distinct alloy-composition related regimes delineated by x=0.3. An attempt is made to link all of this to what is currently known from electronic band structure calculations.

The end-member FeSi is a small gapped semiconductor into which charge carriers are introduced by Co doping [4]. The effect of Co doping (equivalent to iron atom doping plus an additional carrier, e.g., Co = Fe + e^-) is to shift the Fermi level into the conduction band. The internal exchange field from spontaneous magnetic order at $T < T_C$ shifts the two spin bands relative to each other and a redistribution of carriers from one spin channel into the other occurs [14, 28], as seen in figure 4. This effect of the exchange field on the original semiconducting gapped electronic states and fine-structure detail of the bands near E_F, may lead to a scenario in which electrons carrying the majority spin belong to a partially filled metallic band, while those carrying the minority spin involve an empty (at T =0 K) conduction band with E_F in the gap in this spin channel, see x=0.125 in figure 4. The outcome is called a half-metallic ferromagnet in which only one spin channel (majority spins with spin and orbital moments anti-parallel to the exchange field) is responsible for the conduction [28]. This is also deduced from the magnetization behavior (e.g., linear dependence of M_0 on Co composition) [4, 7] and electronic structure calculations [19]. This conduction band is the hybridized 3*d*-4*p* band and, in terms of our XMCD probe, is associated with the x-ray absorbing atom species and next nearest neighboring transition-metal, Fe and Co, sites of the cubic B20 structure. Half-metallicity then implies that there would only be accessible 4*p* states (holes) in one spin channel and the imbalance of empty *p* states with *orbital angular momentum* quantum numbers $+m_l$ and $-m_l$ is quantified by the *K*-edge XMCD integral [18].

It is suggested here that the single peaked nature of the Fe and Co XMCD signals for $x \leq 0.3$ in figure 2, is indicative of holes in only one spin channel near E_F [26]. In positing this we are appealing to what is well known for archetypal transition metal ferromagnets , Fe, Co and Ni.

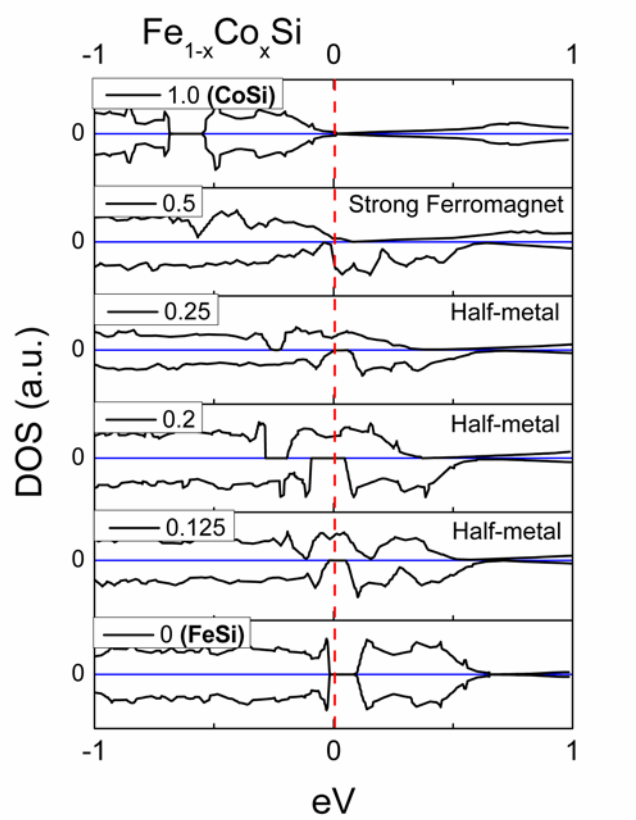

Figure 4 (colour online) : Schematics of electronic band structure (total DOS) in the alloy series, showing the evolution from half metal to strong ferromagnet with increasing Co concentration. Adapted from the *ab initio* band structure calculations of refs [19, 29]. Majority (minority) spin band is in the upper (lower) half of each panel. Fermi energy E_F is at the origin of the horizontal axis.

Electronic structure calculations show that metallic iron (Fe) is a so-called weak ferromagnet with unoccupied 3*d*-4*p* hybridized states at E_F (holes) in both majority and minority spin channels [14]. Electronic structure calculations also reproduce the well known *bipolar* XMCD signature at the *K*-edge [16, 30]. By contrast Co and Ni are so-called strong ferromagnets, having pertinent unoccupied states in only the minority spin channel near E_F and the electronic structure calculations reproduce the characteristic *unipolar K*-edge XMCD. Therefore by analogy with these archetypal ferromagnets magnets, it is contended here that the

unipolar signatures of figures 2(a) and (b) signify unoccupied 3*d*-4*p* hybridized states in only one spin channel. This would be the first experimental elucidation of electronic structure near E_F in these alloy systems, in corroboration of the proposed half metallic nature of the band structure at low doping levels up to x~0.3 in $Fe_{1-x}Co_xSi$ [4, 7, 19], see figure 4. It is a remaining challenge for such *ab initio* calculations of *K*-edge XMCD to be performed for these alloys, in a similar vein to what has been done for Fe and Co elemental ferromagnets [16, 30].

At higher doping levels $x > 0.3$ the XMCD retains its unipolar profile, figures 2(a) and (b), whereas the XMCD integral dependence on Co composition has altered substantially, figures 2(c) and (d). Moreover figure 1 shows that M_0 deviates from linearity and at these high concentrations the original half metallicity at low doping must have evolved to a new scenario. How can all of this be best rationalized ? Drawing on previous electronic structure calculations [29] in conjunction with our XMCD data (figure 2) permits us to make a qualitative description of what has happened. Higher doping *inter alia* shifts E_F to higher energies and there is also likely to be an increase in the exchange splitting. The extent of this is to have moved E_F out of the minority spin band gap up to the majority spin (hybridized 3*d*-4*p*) band edge or beyond that, see x=0.5 in figure 4, with no *3d* hole states available near E_F in this channel. E_F is now rooted in the minority spin channel of the hybridized *3d-4p* conduction band, with accessible states only in this channel for *K*-edge absorption. This is akin to the case of elemental Co or Ni, which exhibit such characteristic strong ferromagnet characteristics as well as unipolar XMCD signatures [14, 16] similar to the profiles in figures 2(a) and (b) for $x \geq 0.3$.

5. Conclusions

We have presented results of an experimental probe of electronic structure near E_F in the $Fe_{1-x}Co_xSi$ series. The Fe- and Co- derived spin polarized (*3d*) bands have been probed, indirectly via the *4p* unoccupied states near E_F, in *K*-edge XMCD experiments. The *K*-edge XMCD presents a unipolar profile for all compositions. The XMCD integral behavior clearly delineates a boundary at x=0.3 and on either side of this the composition dependences of $\langle L_Z \rangle$ are quite different. Differences in the behavior of the composition dependences of the XMCD integral compared with that of the saturation magnetization M_0 and T_C have been ascribed to the spin moment $\langle S_Z \rangle$ contribution, which features only in the latter two quantities.

This is then considered both in conjunction with the most recent electronic band structure calculations and in analogy with the calculated and experimental XMCD signatures in archetypal weak and strong elemental ferromagnets Fe and Co, respectively. It is proposed that x=0.3 in $Fe_{1-x}Co_xSi$ marks a transitioning from half-metallic ferromagnet to strong ferromagnet. The nature of these two ferromagnetic regimes is fundamentally different, although they both entail unoccupied states in only one spin channel and hence, we suppose, manifest as a unipolar profile of the *K*-edge XMCD. Electronic band structure computations specifically of *K*-edge XMCD profiles for these alloy compositions, for comparison with our experimental work, would represent an interesting future challenge. In the half-metallic regime ($x \leq 0.3$) E_F is rooted in the hybridized 3*d*-4*p* majority spin band and is concurrently in a minority spin band *gap*. Whereas in the strong ferromagnet regime E_F is rooted within the 3*d*-4*p* minority spin band and is concurrently at or beyond the majority spin band *edge*. Consequently in this $Fe_{1-x}Co_xSi$ series we may speak of "spin polarization crossover" occurring : from strongly polarized majority spin electron gas in the half-metallic state at $x \leq 0.3$ to minority-spin dominated carriers at higher Co compositions. This information is anticipated to be important for envisioned spintronics applications of these compositions.

Acknowledgements

Funding for this research is derived from the NRF and URC-UJ, and is acknowledged with gratitude. The use of the MPMS system of A.M. Strydom (UJ) for magnetic characterization and part of the data processing by L. Nataf (SOLEIL), is also acknowledged with thanks.

References

[1] M. Fanciulli, A. Zenkevich, I. Wenneker, A. Svane, N. E. Christensen and G. Weyer, Phys. Rev. B 54 (1996) 15985

[2] K. Shimizu, H. Maruyama, H. Yamazaki and H. Watanabe, J. Phys. Soc. Jpn 59 (1990) 305

[3] J. Beille, J. Voiron and M. Roth, Solid State Commun. 47 (1983) 399

[4] Y. Onose, N. Takeshita, C. Terakura, H. Takagi and Y. Tokura, Phys. Rev. B 72 (2005) 224431

[5] S. V. Grigorieva, V. A. Dyadkina, S. V. Maleyeva, D. Menzel, J. Schoenes, D. Lamagoc, E. V. Moskvina and H. Eckerlebed, Physics of the Solid State 52 (2010) 907.

[6] Unravelling of the helical spin structure and transition from a conical to ferromagnetic state occurs at low applied fields not exceeding 0.2 T, depending on Co concentration *x*. Magnetization values reach plateau (saturation like) values by 0.2 T, although there is still a weak increase in value to higher fields of 9 T. The weak slope varies somewhat from low to high Co doping regimes.

[7] N. Manyala, Y. Sidis, J. F. DiTusa, G. Aeppli, D. P. Young and Z. Fisk, Nature 6 (2000) 581

[8] J. P. DeGrave, A. L. Schmitt, R. S. Selinsky, J. M. Higgins, D. J. Keavney and S. Jin, Nano Lett. 11 (2011) 4431

[9] N. Manyala, Y. Sidis, J. F. Ditusa, G. Aeppli and D. P. Young, Nature Mater. 3 (2004) 255

[10] N. A. Porter, G. L. Creeth and C. H. Marrows, Phys. Rev. B 86 (2012) 064423

[11] J. M. Tomczak, K. Haule and G. Kotliar, PNAS 109 (2012) 3243.

[12] S. Kawarazaki, H. Yasuoka, Y. Nakamura and J. H. Wernick, J. Phys. Soc. Japan 41 (1976) 1171

[13] *L*-edge dichroism is a more direct probe of the pertinent *3d* states, although it is more surface sensitive and we are interested in an effective probe of the bulk magnetic-electronic properties for which *K*-edge investigations may be better suited, see M. Sikora, A. Juhin, T-C Weng, P. Sainctavit, C. Detlefs, F. de Groot and P. Glatze, Phys. Rev. Lett. 105 (2010) 037202.

[14] J. Stöhr and H. C. Siegmann, Magnetism: From Fundamentals to Nanoscale Dynamics (Springer-Verlag, Berlin Heidelberg, 2006).

[15] C. Brouder and M. Hikam, Phys. Rev. B 43 (1991) 3809

[16] I. Igarashi and K. Hirai, Phys. Rev. B 50 (1994) 17820

[17] V. N. Antonov, B. N. Harmon and A. N. Yaresko, Phys. Rev. B 67 (2003) 024417

[18] G. Y. Guo, J. Phys.: Condens. Matter 8 (1996) L747.

[19] J. Guevara, V. Vildosola, J. Milano and A. Llois, Phys. Rev. B 69 (2004) 184422

[20] I. I. Mazin, App. Phys. Lett. 77 (2000) 3000

[21] M. P. J. Punkkinen, K. Kokko, M. Ropo, I. J. Väyrynen, L. Vitos, B. Johansson and J. Kollar, Phys. Rev. B 73 (2006) 024426

[22] A. Monza, A. Meffre, F. Baudelet, J.-P. Rueff, M. d'Astuto, P. Munsch, S. Huotari, S. Lachaize, B. Chaudret and A. Shukla, Phys. Rev. Lett. 106 (2011) 247201

[23] F. Baudelet, S. Pascarelli, O. Mathon, J.-P. Itié, A. Polian and J.-C. Chervin, Phys. Rev. B 82 (2010) R140412

[24] Absorption of these incident photons results in corresponding *spin-polarized photoelectrons* for "detecting" (i.e., populating) majority/minority spin holes, $N_h^{m_s}$, in the 4*p* conduction band where m_s is the electron spin quantum number. Thus spin polarized x-ray absorption spectra (or spin dependent absorption coefficients) μ^+ and μ^- are recorded, from

which the dichroism signal may be obtained (i.e. , $\mu^+ - \mu^-$). A normalized spin-dependent absorption profile $(\mu^+ - \mu^-) / (\mu^+ + \mu^-)$ is computed from the absorption spectra so as to obtain the thickness-independent XMCD for inter-comparison across the alloy series.
[25] S. Stähler, G. Schütz and H. Ebert, Phys. Rev. B 47 (1993) 818
[26] S. Pizzini, A. Fontaine, C. Giorgetti, E. Dartyge, J. Bobo, M. Piecuch and F. Baudelet, Phys. Rev. Lett. 74 (1995) 1470
[27] The interval of integration has been over 50 - 60 eV encompassing the XMCD signal peak. The background is obtained by integration over 50 - 60 eV far from the edge and subtracted from the preceding integral of the signal. These operations were repeated for different data processing procedures (e.g., by changing the interval used), to provide an estimate of the error incurred in the data reduction.
[28] F. P. Mena, J. F. DiTusa, D. v. d. Marel, G. Aeppli, D. P. Young, A. Damascelli and J. A. Mydosh, Phys. Rev. B 73 (2006) 085205
[29] H. Zhi-Hui, H. Wei, S. Young and C. Zhao-Hua, Chinese Phys. 16 (2007) 3863.
[30] G. Y. Guo, Phys. Rev. B 55 (1997) 11619